Human Cord Blood-Derived Unrestricted Somatic Stem Cell Infusion Improves Neurobehavioral Outcome in a Rabbit Model of Intraventricular Hemorrhage

GOVINDAIAH VINUKONDA [ID],[a,b,*] YANLING LIAO,[a] FURONG HU,[a] LARISA IVANOVA,[a] DEEPTI PUROHIT,[c] DINA A. FINKEL,[c] PRIYADARSHANI GIRI,[c] LAKSHMIPRAMODA BAPATLA,[b] SHETAL SHAH,[a,c] MUHAMMED T. ZIA,[c] KAREN HUSSEIN,[a,c] MITCHELL S. CAIRO [ID],[a,b,d,*] EDMUND F. LA GAMMA[a,e,c,*]

Key Words. Locomotor function • Bioluminescence imaging • Intraventricular hemorrhage • Unrestricted somatic stem cells (USSCs) • White matter injury • Myelination

[a]Department of Pediatrics, New York Medical College, Valhalla, New York, USA; [b]Cell Biology & Anatomy, New York Medical College, Valhalla, New York, USA; [c]The Regional Neonatal Center at Maria Fareri Children's Hospital of Westchester Medical Center, Valhalla, New York, USA; [d]Department of Medicine, Pathology, Microbiology & Immunology, Cell Biology & Anatomy, New York Medical College, Valhalla, New York, USA; [e]Department of Biochemistry and Molecular Biology, New York Medical College, Valhalla, New York, USA

*Co-senior authors.

Correspondence: Govindaiah Vinukonda, Ph.D., Departments of Pediatrics and Cell Biology & Anatomy, New York Medical College, Valhalla, New York 10595, USA. Telephone: 914-594-4661; e-mail: g_vinukonda@nymc.edu

ABSTRACT

Intraventricular hemorrhage (IVH) is a severe complication of preterm birth, which leads to hydrocephalus, cerebral palsy, and mental retardation. There are no available therapies to cure IVH, and standard treatment is supportive care. Unrestricted somatic stem cells (USSCs) from human cord blood have reparative effects in animal models of brain and spinal cord injuries. USSCs were administered to premature rabbit pups with IVH and their effects on white matter integrity and neurobehavioral performance were evaluated. USSCs were injected either via intra-cerebroventricular (ICV) or via intravenous (IV) routes in 3 days premature (term 32d) rabbit pups, 24 hours after glycerol-induced IVH. The pups were sacrificed at postnatal days 3, 7, and 14 and effects were compared to glycerol-treated but unaffected or nontreated control. Using in vivo live bioluminescence imaging and immunohistochemical analysis, injected cells were found in the injured parenchyma on day 3 when using the IV route compared to ICV where cells were found adjacent to the ventricle wall forming aggregates; we did not observe any adverse events from either route of administration. The injected USSCs were functionally associated with attenuated microglial infiltration, less apoptotic cell death, fewer reactive astrocytes, and diminished levels of key inflammatory cytokines (TNFα and IL1β). In addition, we observed better preservation of myelin fibers, increased myelin gene expression, and altered reactive astrocyte distribution in treated animals, and this was associated with improved locomotor function. Overall, our findings support the possibility that USSCs exert anti-inflammatory effects in the injured brain mitigating many detrimental consequences associated with IVH. STEM CELLS TRANSLATIONAL MEDICINE 2019;8:1157–1169

SIGNIFICANCE STATEMENT

Intraventricular hemorrhage (IVH) is a common complication of premature newborns associated with white matter injury, cerebral palsy, and mental retardation. Currently, there are no therapies for this condition, which affects approximately 12,000 babies every year in the U.S. This article reports that cord blood-derived cells delivered in preterm rabbits with IVH decrease microglia infiltration, pro-inflammatory cytokines, and apoptotic cell loss. Cell treatment led to a partial recovery of myelination, preservation of white matter, and resumption of motor function. These findings support the notion that cord blood-derived stem cells have therapeutic potential for the treatment of degenerative processes caused by IVH.

INTRODUCTION

The germinal matrix (GM) is the site of proliferating neuronal and glial precursor cells in the developing brain. Germinal matrix hemorrhage (GMH)-intraventricular hemorrhage (IVH) is a severe complication of preterm birth and is characterized by hemorrhagic injury in the subependymal region with resultant rupture into the lateral ventricle. The incidence of IVH in premature infants with birth weight under ≤1,500 g approximates 20%. [1, 2] Despite improvements in obstetrical care, the rate of preterm birth has begun to increase again, which will potentially result in an increased prevalence of IVH. [1, 3] Common consequences

of IVH-mediated white matter injury include the development of hydrocephalus, cerebral palsy, and mental retardation. [4, 5] Diffuse "hypomyelination and gliosis" are the most common white matter lesions reported with an elevation of pro-inflammatory cytokines, including IL-1β and TNFα, and also implicated in the pathogenesis of white matter injury, including ischemic and traumatic brain injuries. [6, 7] Currently, there are no preventive therapies for IVH; cell-based therapies represent a new hope of intervention for the rescue of pathologies that develop after IVH in premature birth.

Two animal models of IVH are previously reported: (a) injection of *exogenous* blood into the ventricles of newborn rodents [8–11] and (b) our model of intraperitoneal glycerol-induced *endogenous* IVH in premature rabbit pups. [12–16] We prefer the glycerol-induced endogenous IVH model as rabbit brains closely approximate human stages [17, 18] as well as replicate many of the clinical manifestations of IVH seen in premature human neonates including hypomyelination, gliosis, pro-inflammatory cytokines, apoptosis as well as spastic diplegia, neurodegeneration, and cognitive delays. [13, 14, 19, 20] Prior preclinical investigations using mesenchymal stem cells (MSCs) in the injected exogenous blood rodent model of IVH showed improved myelination, neuroprotection. [9–11] Beneficial effects arose primarily via paracrine anti-inflammation pathways rather than from true engraftment, regeneration, or differentiation. [8, 10, 11]

Kogler et al. isolated a novel nonhematopoietic multipotent stem cell population from human umbilical cord blood unrestricted somatic stem cells (USSCs). These cells have the ability to differentiate into all germ layers both in vitro and in vivo. [21] USSCs share overlapping cell surface markers with MSCs; however, USSCs can be distinguished from MSCs by broader differentiation capacity and differential expression of genes. [21–24] USSCs also release growth factors with known neuroprotective and axon growth promoting functions at higher levels than MSCs, such as leukemia inhibitory factor (LIF), vascular endothelial growth factor (VEGF), [25, 26] and stromal cell-derived factor-1 which induces homing of neural stem cells to ischemic brains [22, 27] plus stimulates axonal sprouting after spinal cord injury. [28] USSCs also release hepatocyte growth factor, which is known to promote motor neuron survival and axonal regrowth, and is a guidance and survival factor during neural development. [29, 30]

In previous studies, our group engineered USSCs to express the luciferase reporter gene, confirmed a stable non-teratogenic phenotype, and then successfully tracked USSC migration in a living animal model of recessive dystrophic epidermolysis bullosa (RDEB) and in excisional wounding healing. [24, 31] In the RDEB model, USSC administration migrated to the site of injury and suppressed TGFβ signaling-mediated fibrosis and attenuated inflammatory cytokine expression (IL6, IFNγ, and IL17α). [32]

The goal of the present pilot study was to investigate the therapeutic potential of USSCs in a premature rabbit pup model of glycerol-induced IVH. [12–14] We investigated two routes of USSC administration (directly into the cerebral ventricles, intracerebroventricular [ICV] and systemically via the jugular vein, intravenous [IV]) and examined the migration of USSCs in living animals followed by their impact on white matter injury and motor recovery. USSCs reduced inflammatory markers and improved both myelination and motor performance in rabbit pups with IVH, using either route of cell delivery.

METHODS

Preparation of Cord Blood Derived USSCs

USSCs were isolated from fresh human umbilical cord blood mononuclear cells based on outgrowth of spindle-shaped colonies in the presence of low glucose DMEM, 30% FBS, 10^{-7} M dexamethasone, penicillin/streptomycin, and 2 mM ultraglutamine and cultured in the same medium without dexamethasone according to the methods of Kogler as we previously described. [21, 24] USSCs were transduced with lentivirus carrying GFP-luciferase gene prepared using lentiviral construct, pSico PolII-eGFP-Luc2, generously provided by Glenn Merlino at the National Cancer Institute, where the cells retained their functionality. [24] The transduced USSCs were validated based on cell surface markers, expression of DLK1 and lack of expression of HOX gene clusters. USSCs were expanded at 5–8 passages following our published method and were used in this study. [24]

Glycerol-Induced GMH-IVH in Premature Rabbits

Timed pregnant New Zealand white rabbits were purchased from Charles River Laboratories Inc. (Wilmington, MA) and premature rabbit pups were delivered by cesarean section at E29 gestational age (term gestation = 32 days). Newborn pups were maintained and fed accordingly with our previously published methods. [13, 19] At 3–4 hours of postnatal age, newborn pups were treated with 50% intraperitoneal glycerol: water (6.5 g/kg) which induced IVH in approximately 70% of all treated animal pups. [13, 19] Head ultrasound was performed at 24 hours postnatal age to determine the presence and severity of IVH (Acuson Sequoia C256, ultra-sonographic Imaging System [Siemens Corp., Washington, DC]). The grades of IVH pups were classified based as: (a) no gross IVH, (b) moderate, gross hemorrhage, or (c) severe IVH filling both ventricles completely. [13] All interventions were approved by New York Medical College Institutional Animal Care and Use Committee.

USSC Administration and In Vivo Bioluminescence Imaging (BLI)

For ICV *injection*, at 24 hours of postnatal age (20 hours after glycerol), a single dose of 2 million USSCs (1×10^6 cells/ventricle in 10 μl) was injected directly into each lateral ventricle under stereotaxic guidance, following coordinates from Bregma: 1 mm posterior, 4 mm lateral and 3 mm deep. For IV administration, USSCs were injected via the jugular vein at a total dose of 1×10^6 cells/dose mixed in to 150 μl saline. Volume-matched saline injections were performed in IVH controls. The condition of rabbit pups after hemorrhage and USSC infusion was assessed and monitored twice a day for suffering and weight gain. The rabbit pups that received USSC administration were imaged by performing bioluminescence imaging using a Xenogen IVIS imaging system (Hopkinton, MA), for USSC trafficking and persistence in vivo. To accomplish this, pups were anesthetized with isoflurane (Phoenix Pharmaceutical Inc.) and injected intraperitoneally with substrate 50 mg/kg of XenoLight rediJect D-Luciferin Ultra, (Caliper, Hopkinton,

MA) 15 minutes before imaging. Live images were taken at days 1, 3, 7, and 14, respectively. The total photon emission from each rabbit pup at each time point was quantified to determine the dynamics of USSC persistence in vivo. Subsets of pups were electively sacrificed after each imaging time point and tissue samples were collected and processed for analysis.

Assessment of Rabbit Cytokines Using Quantitative RT-PCR

The mRNA expression was performed by real-time PCR as previously described. [14, 20, 33] Briefly, total RNA was isolated using an RNeasy Mini kit (catalog # 74104, QIAGEN) from a coronal brain slice taken at the level of the mid-septal nucleus. cDNA was synthesized using Superscript II RT enzyme (catalog # 05081955001, Roche, Indianapolis, IN) followed by real-time quantification using SYBR green method (catalog # 04913850001, Roche). The same primer sets were used as described previously. [14, 33] Analysis was completed using the efficiency corrected $\Delta\Delta CT$ method and the data were presented in percentages. [34]

Protein Blot Analyses

Glial fibrillary acidic protein (GFAP) blot analyses was performed using our previously described method [20, 33] after protein homogenates was made from fore-brain coronal slices were taken at the level of mid-septal nucleus from the three experimental groups. The primary antibodies used in the experiments included mouse monoclonal GFAP (catalog # G6171, St. Louis, MO). The same blot was stripped with stripping buffer and probed with mouse monoclonal β-actin primary antibody (catalog # A5316) followed by secondary antibody and detected with ECL system. [14] As described previously, [33] the blots from each experiment were analyzed densitometrically using ImageJ software (NIH.gov); optical density values were normalized to beta actin.

Immunohistochemistry (IHC)

Immunohistochemical staining was performed as we previously described. [12, 14, 33] Briefly, the tissue was fixed in 4% paraformaldehyde and blocks were made in optimal cutting temperature followed by coronal sectioning at the level of 1.0 mm anterior to 1.0 mm posterior of bregma. The fixed sections were hydrated in 0.01 M phosphate buffered solution and incubated with the primary antibodies overnight at 4°C followed by a secondary antibody for 1 hour at room temperature. After washing, the sections were mounted with mounting media—slow fade Light Anti-fade reagent (Molecular probes, Invitrogen, Carlsbad, CA, http://www.invitrogen.com)—and then visualized microscopically.

Anatomical Localization of ICV and IV-Routed USSCs

To confirm the presence and anatomical location of migrated USSCs in rabbit tissue at different postnatal ages, sections were stained using antihuman nuclei (hNuc) antibody (cat # MAB 1218, EMD Millipore, Billerica, MA, http://www.millipore.com) and counter stained with diamidino-phenylindole (DAPI). Signals for immunoreactivity were imaged using a fluorescence microscope (Nikon Eclipse-90i with the NIS Element software Nikon Instruments, Japan) in ×4/×10/×40 images.

Quantification of Apoptotic Cell Death and Microglial Cell Density

To investigate the effect of USSC infusion on cell death and microglial infiltration on coronal brain sections, we counterstained sections with propidium iodide (PI)/DAPI nuclear staining at postnatal day 3. Since the brain hemorrhage and resultant cellular infiltration plus apoptosis are nonuniform around the ventricle, we counted positive cells in the entire subventricular zone (SVZ) and periventricular zone in the GM, corona radiata (CR), and corpus callosum (CC). For *cell death*, the number of terminal transferase-mediated dUTP nick-end labeling (TUNEL) positive cells was counted following manufacturer's protocol (apoptosis Kit Cat # 17-141; EMD-Millipore/Sigma). We performed TUNEL positive cell counting on fixed sections as described previously. [14, 19] Microglia cell density was assessed using Iba-1 specific antibody (catalog # AB5076, Abcam, Cambridge, U.K., http://www.abcam.com) as we and others previously described. [35, 36] A blind cell count was performed by two investigators to determine the cell density using ImageJ software with grid. We counted four sections in each pup and 5–6 pups from each group. Data are presented as mean cell count (mean $\pm$ SEM).

Neurobehavioral Examination

Neurological testing was performed at postnatal day 14 using previously described scoring systems. [13, 14, 19, 20, 37] Evaluations were performed independently by two investigators (Furong and Zia) blinded to the group assignment. The end points included (a) Tone: scoring with modified Ashworth's scale; (b) Posture: evaluation of standing posture and trunk; and (c) Locomotor function: Locomotion at 30° inclinations, ability to hold at 60° slopes, walk and hopping (latency to slip down a slope), righting reflex, and gait. We graded the responses on a scale of 0–3 (0 being the worst response and 3, the best) in all experimental groups.

Statistics and Analysis

Data are expressed as means $\pm$ SEM. To determine differences in cell counts between the four groups, we used one-way ANOVA to compare groups. Gene expression for cytokines between the groups at day 3 was compared by two-way ANOVA. All post hoc comparisons were done using Tukey's multiple comparison testing and *p*-values ≤.05 were considered significant.

RESULTS

USSC Administration Improved Locomotor Function and Neurological Impairment in Rabbit Pups with IVH

To evaluate whether USSC administration yielded functional improvement in rabbit pups with IVH, we evaluated motor and sensory function in the four experimental groups at day 14 (Table 1). In our prior work, we reported that the glycerol-induced IVH in premature rabbit pups caused white matter injury seen histologically as hypomyelination and astrogliosis that was associated with sensorimotor impairment. As expected, compared to the no IVH group, the IVH-saline controls were severely impaired in motor activity (Table 1; $p < .05$). IVH pups were paralyzed due to spastic diplegia, as

Table 1. USSC administration improved locomotor function and neurological impairment in IVH pups compared to IVH saline controls at postnatal day 14. Table for neurobehavioral scores of pups with no IVH, and IVH pups with and without USSC administration. The comparisons done at postnatal day 14

System	Test performed	No IVH (n = 12)	IVH saline (n = 8)	IVH-USSC IV (n = 6)	IVH-USSC ICV (n = 9)
Cranial nerve	Response to alcohol	3 (3,3)	3 (3,3)	3 (3,3)	3 (3,3)
	Sucking and swallowing	3 (3,3)	3 (3,3)	3 (3,3)	3 (3,3)
Motor function	Head	3 (3,3)	3 (2.5,3)	3 (3,3)	3 (3,3)
	Fore legs	3 (3,3)	3 (2.7,3)	3 (3,3)	3 (3,3)
	Hind legs	3 (3,3)	3 (2.1,3)[#]	3 (3,3)*	3 (3,3)*
	Righting reflex[a]	5 (5,5)	4 (1.5,5)[#]	5 (5,5)*	5 (5,5)*
	Locomotion on 30° inclination[b]	3 (3,3)	3 (1,3)[#]	3 (3,3)*	3 (3,3)*
	Tone[c]: Fore limb	0 (0,0)	0 (0,0)	0 (0,0)	0 (0,0)
	Tone[c]: Hind limb	0 (0,0)	0 (0,0)	0 (0,0)	0 (0,0)
	Inability to hold their position at 60°	0%	34%	11%	8%
	Distance walked in 60 seconds (inches)	102 ± 33	32.5 ± 17[#]	85 ± 12.9*	81.2 ± 30*
	Gait[d]	4 (4, 4)	3 (1.5, 3)[#]	4 (3.5, 4)*	4 (4, 4)*
	Motor impairment[e]	0%	51%[#]	12%*	7%*
Sensory	Facial touch	3 (3,3)	3 (3,3)	3 (3,3)	3 (3,3)
	Pain	3 (3,3)	3 (3,3)	3 (3,3)	3 (3,3)

Values are median (interquartile range). Zero is the worst response and 3 is the best response, unless otherwise noted.
[a]Score (range 1–5): number of times turns prone within 2 seconds when placed in supine out of 5 tries.
[b]Score (range 0–3): 0, does not walk; 1, takes a few steps (less than 9 inches); 2, walks for 9–18 inches; 3, walks very well beyond 18 inches.
[c]Score (range 1–3): 0, no increase in tone; 1, slight increase in tone; 2, considerable increase in tone; 3, limb rigid in flexion or extension.
[d]Gait was graded as 0, no locomotion; 1, crawls with trunk touching the ground for few steps and then rolls over; 2, walks taking alternate steps, trunk low and cannot walk on inclined surface; 3, walks taking alternate steps, cannot, but walks on 30° inclined surface; 4, walks, runs, and jumps without restriction; 5, normal walking.
[e]Motor impairment was defined as weakness in either fore legs or hind legs and distance walked <60 inches in 60 seconds. [#]$p < .05$, for no IVH versus IVH saline vehicle controls. *$p < .05$, for IVH saline vehicle versus ICV, IV USSC injected IVH pups. Walking distance in mean ± SEM).
Abbreviations: ICV, intracerebroventricular; IV, intravenous; IVH, intraventricular hemorrhage; USSC, unrestricted somatic stem cell.

well as demonstrated abnormal righting reflex and posture/gait (Supporting Information Video S1). Moreover, they developed hydrocephalus with a ventricular area 5.93 ± 0.34 mm^2 in controls versus 34.27 ± 6.23 mm^2 in IVH pups ($p < .05$). Importantly, USSC administration (either ICV or IV) significantly improved the average scores for motor activity of the limbs in pups with IVH (Table 1). Both groups of IVH-USSC treated animals (ICV and IV) recovered to near normal posture/gait and did not develop severe hydrocephalus as evident from a ventricle area 14.93 ± 4.51 mm^2 for ICV treatment and 10.88 ± 5.23 mm^2 IV treatments.

Of note, treatment with USSCs in IVH-affected animals improved walking distance. Five of eight IVH pups demonstrated significantly reduced walking distance compared to the controls ($p < .05$), whereas 5 of 6 IV injected pups and 7 of 9 ICV injected pups showed significantly improved walking distance compared to IVH pups ($p < .05$). We did not find any other adverse behavior such as respiratory distress in rabbit pups after USSCs injection by either route. The animals were video recorded to illustrate overall motor function and gait/posture, which can be viewed at Video S1.

Dynamics of USSC Migration and Anatomic Localization in Rabbit Pups with IVH

The similar extent of improvement in the sensorimotor outcome after either route of USSC administration led us to investigate the migration and anatomic localization of USSCs, using

complementary methods of BLI based on the luciferase reporter gene in USSCs and human nuclei-specific IHC staining. BLI was performed in live animals after USSC administration at postnatal days 1, 3, 7, and 14 with 5–6 pups examined at each time point (Fig. 1). In the ICV group, the BLI signal was stable in the first few days, became significantly diminished at day 7, and was barely detectable on day 14 (Fig. 1A, 1D). As expected, BLI was detected from the extracted whole brain and coronal brain slices at day 3 (Fig. 1B, 1C). The little or no bioluminescence on day 14 was likely due to insufficiency of photon transmission through the developing rabbit skull or due to slow cell death and/or further migration of USSCs.

We also used BLI to monitor the migration of USSCs in rabbits with IVH after IV injection. The bioluminescent signal accumulated in the lung at early time points, represented by the day 3 BLI in Figure 1E. At this time point, foci of bioluminescence emitting from the hemispheres of the brain were also apparent and the level of total photon influx in the brain (6.29E+05 ± 1.6E+5 p/s; n = 5) was approximately half the level present in the lung (1.25E+6 ± 3.44E+5 p/s; n = 5) (Fig. 1E). Importantly, the bioluminescence persisted in the brain on day 7, even though the signal in the lung was significantly decreased to a background level. On day 9, there was a further decrease of the bioluminescent signal in the brain. As mentioned above, this decrease of the bioluminescence could be related to the increased bone thickness and density in the skull with age. Nevertheless, bioluminescence was still noticeable in the rabbit
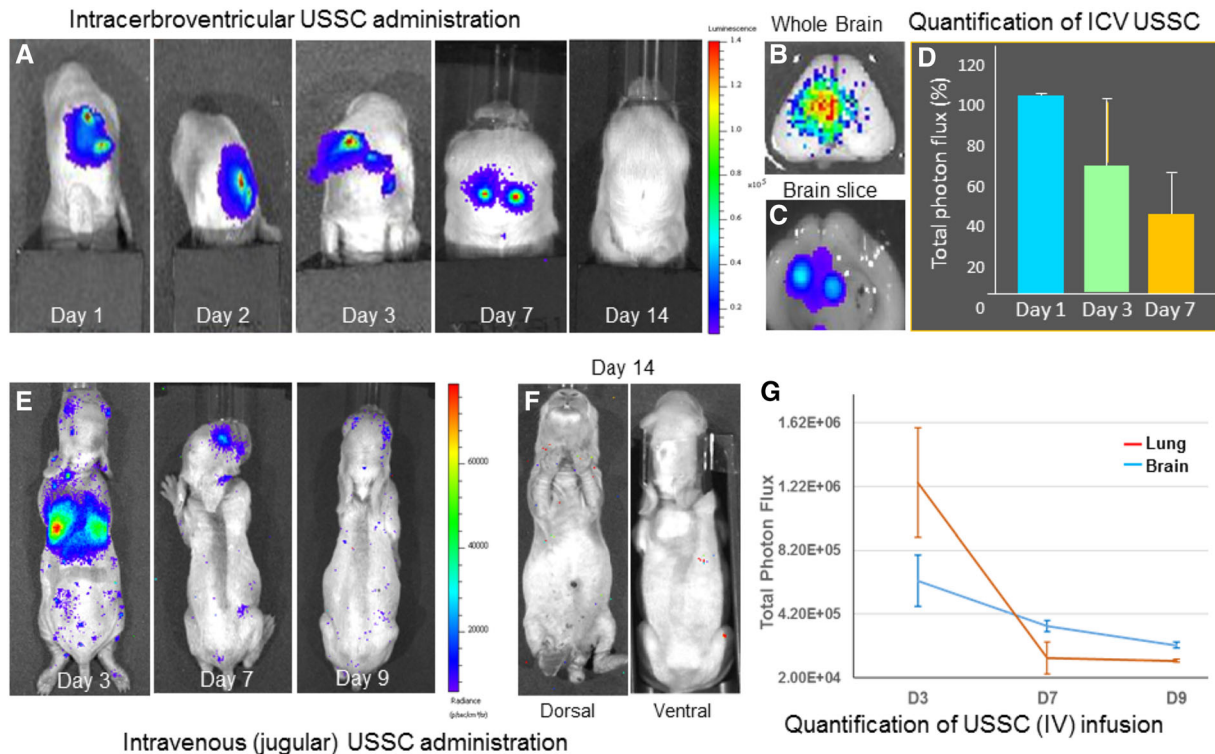
Figure 1. Bioluminescence live images (BLI) of USSC engraftment by ICV and IV routes of delivery in IVH pups. **(A):** BLI live images of IVH pups following single dose of ICV USSC (2×10^6 cells/dose) injection of luciferase-labeled USSC. Stable signals were obtained until postnatal days 1–7, and indicated live and healthy USSCs. Furthermore, USSCs were barely detectable or no detection was observed at postnatal day 14. **(B, C):** BLI signal in whole brain and coronal brain slice dissected from day 3 USSC-injected IVH pup. A dispersed luminescent signal in the brain indicates further migration of USSCs (200 μm slice). **(D):** Quantification of total photon flux on days 1, 3, and 7 of IVH pups following luciferase (pSico PolII-eGFP-Luc2) labeled USSCs injections indicates a steady decrease in BLI signal over time. **(E):** Representative days 3, 7, and 9 BLI on a rabbit pup with IVH that received USSCs via a jugular vein injection demonstrating migration of USSCs to the brain after transient retention in the pulmonary circulation; IV USSC cleared from the lung by day 7 after infusion (1×10^6 cells/dose). **(F):** Day 14 BLI of a rabbit with IVH that received IV USSCs illustrating no cell persistence in the lung or other organs (dorsal and ventral views). The same color bar was applied to all the four images. **(G):** Quantitation on the total photon flux from the brain and lung regions at postnatal days 3, 7, and 9 in the rabbit pups with IVH. The pups were anesthetized with isoflurane and injected intraperitoneal substrate 50 mg/kg of XenoLight rediJect D-Luciferin Ultra (Caliper) 15 minutes before imaging and all images were taken at same threshold of sensitivity. Abbreviations: ICV, intracerebroventricular; IV, intravenous; USSC, unrestricted somatic stem cell.

brain with IVH at that time point. Further follow-up of IV injected USSCs by day 14 showed no BLI signals in lung as well as all other organs in the whole animal imaging (Fig. 1F). These results demonstrated the ability of USSCs to migrate from the systemic circulation into an IVH brain.

To trace the precise migration and anatomical localization of ICV injected USSCs, cells were identified by IHC staining using the specific nuclear antigen (Fig. 2). In coronal sections stained from ICV injected IVH pups, USSCs formed rosette-like structure in the ventricle on day 3 and lined up along the edges of the aggregates approaching the ventricular wall (Fig. 2A, 2B); by day 7, USSCs invaded the surrounding ventricular wall (Fig. 2C, 2D). Importantly, by day 14, the ICV injected USSCs, showed no further evidence of ventricular aggregates and had clearly moved into the subventricular area (Fig. 2E, ×4) also dispersing into the SVZ (Fig. 2F, ×20). "We also performed immunohistochemical staining on the lung section. No human cells were identified in the lung between day 1 to day 3 post USSC administration (data not shown), even though BLI indicated the presence of USSCs in the lung. This suggests that most of the human cells were in the blood circulation of the

lung vasculature rather than integration into the lung epithelium at an early time points. However, human cells were indeed identified in the lung at day 7 and 14 post USSC administration (Fig S3 lower panel). The mechanism underlying this observation is currently under an independent investigation." We also observed USSCs at different locations around the ventricular wall, including the choroid plexus and hippocampus (Fig. S1A–S1E).

In comparison to the ICV route, IV-injected USSCs detected by immunostaining were more evenly distributed through the periventricular region in forebrain sections at day 3 (Fig. S2A, S2B) than at later postnatal days 7 and 14 (Fig. S2C–S2F). During the later days, substantial migration of USSCs to the ventricular zone had occurred (Fig. S2E, ×10 and S2F, ×20). Importantly, we found that IV-injected USSCs migrated to the choroid plexus in the ventricles by day 14 (Fig. S3, upper panel). A few USSCs were also present in the lung sections at days 7 and 14 (Fig. S3, lower panel). We did not find USSCs by BLI or by IHC sections from liver, kidney, heart, and intestines, which suggest the absence of USSC migration to these unaffected peripheral organs.
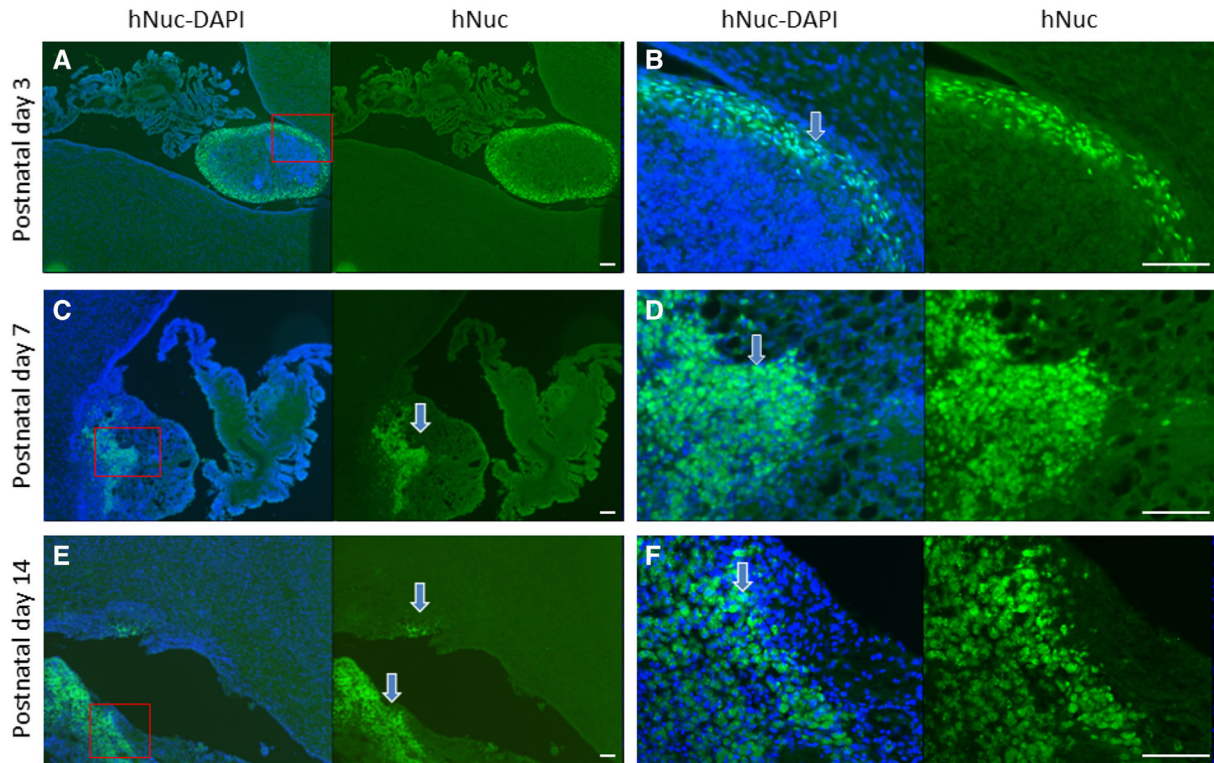
Figure 2. Representative immunofluorescence images of cryosections for tracking intracerebroventricular (ICV)-delivered unrestricted somatic stem cell (USSC) in intraventricular hemorrhage (IVH) pups. **(A, B):** Representative immunofluorescence images for USSCs tracking using human-specific nuclear antibody. The human-specific immunoreactivity of USSCs appeared as aggregates on day 3 in the ventricle approaching toward ventricle wall. Anatomical area of USSCs boxed and magnified as shown in low and high magnification. **(C, D):** Images for day 7 and **(E, F)** images for day 14. Note that USSCs were present with elongated nucleus in migratory phase and cells migrated further deeper ventricular area by day 14. The sections were counter stained with DAPI (stains both rabbit and human cells). The down arrow shows USSCs. Scale bar for all images 100 μm, ICV USSC: 2×10^6 cells/dose. Abbreviations: DAPI, diamidino-phenylindole; hNuc, human-specific nuclear.

USSC Administration Reduced Endogenous Cell Death and Microglial Infiltration

To assess the extent of apoptotic cell death, we performed TUNEL staining on fixed cryosections at day 3 with 5–6 pups in each group. Consistent with our prior reports, [14, 19] the number of TUNEL positive cells in the ventricular area (GM, CR, and CC) was higher in the IVH group compared with the controls at day 3 (Fig. 3A, 3E and 3B, 3F). Notably, the IVH pups injected with USSCs by either route of administration showed reduced TUNEL positive cells compared to IVH-saline controls (Fig. 3C, 3G and 3D, 3H). The sections were co-stained with PI to identify nuclei that were co-localized with TUNEL positive cells. The quantification of apoptotic cells was significantly higher on day 3 in IVH pups compared to controls (p = .01). In contrast, USSC administration significantly reduced cell death compared to IVH controls at day 3 (p < .05; Fig. 3I). These results suggest USSC administration by either route suppressed IVH-triggered apoptosis in rabbit pups.

To assess the effect of USSCs on progression of inflammation during IVH, we quantified microglia in the experimental groups at day 3. Immunoreactivity of microglia using the specific Iba-1 antibody was higher in the IVH group compared with no IVH controls in the CR and GM (Fig. 3J, 3K). In contrast, ICV-administered USSC pups showed reduced immunoreactivity for microglia compared to the IVH group (Fig. 3L). We

then assessed the density of microglia in the ventricular area in three groups (no IVH, IVH-saline, and IVH-ICV USSC pups). The mean density of microglia was significantly increased in IVH pups compared with controls (IVH-saline: 252 ± 46 mm^2 vs. controls: 122 ± 25 mm^2, p < .05). Furthermore, the microglia were diminished in the ventricular area of the USSC injected pups with IVH (IVH-saline: 252 ± 46 mm^2 vs. IVH-USSC 185 ± 41 mm^2, p < .05).

USSC ICV Administration Increases Myelin Gene Expression Followed by Improved Myelination After IVH

Since IVH causes reduced myelination, we asked whether USSC administration altered the myelination process in the hemorrhagic brain. As shown in coronal brain slices (Fig. S4), the major bleeding in our rabbit model was evident in the GM (Fig. S4E–S4J) and extended to surrounding CR and CC of the white matter region. To assess the magnitude of white matter injury, we evaluated the morphological changes of myelin fibers in the CR by immunolabeling myelin basic protein (MBP) at day 14 (Fig. 4A–4F). Expression of MBP in the CR was reduced in IVH pups compared to controls without IVH (Fig. 4A, 4B vs. 4C, 4D). The myelin fibers in the IVH group were reduced, small, and thin in morphological appearance, similar to our previous reports (Fig. 4C, 4D). In contrast,
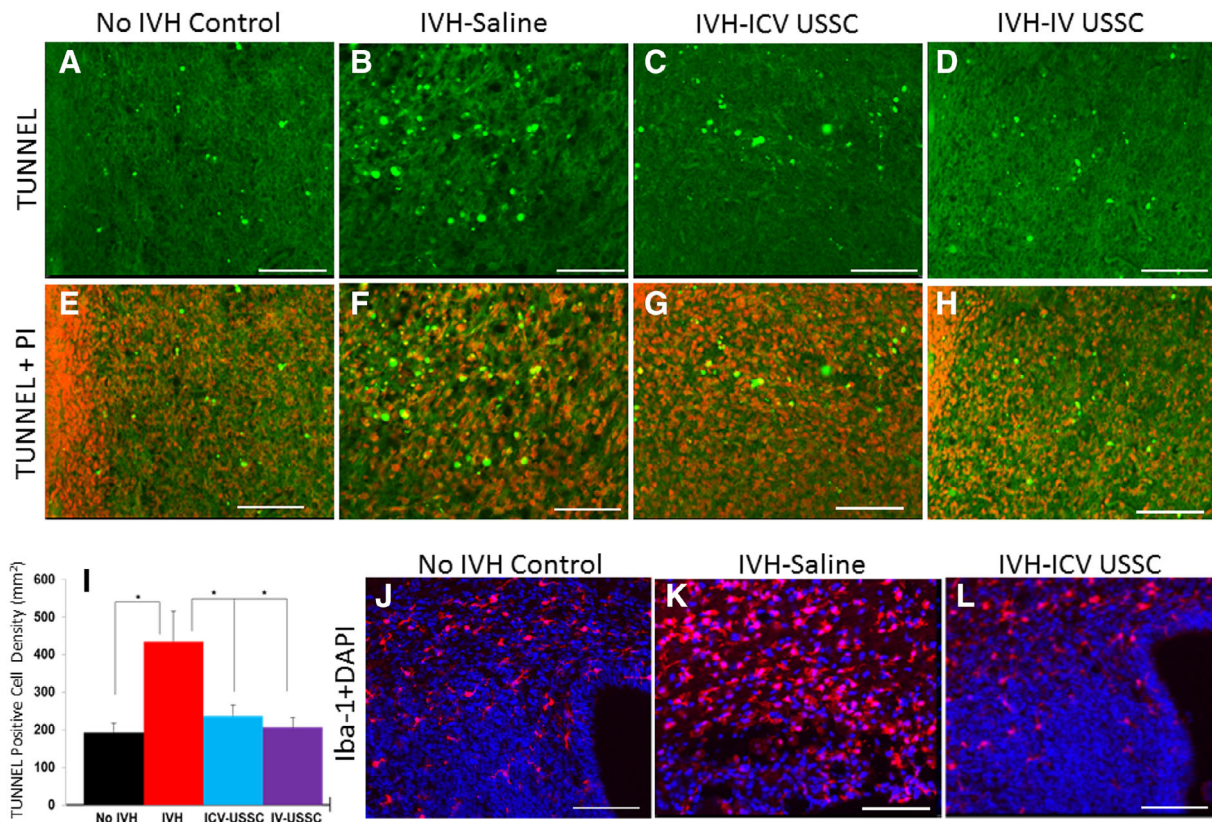
Figure 3. Reduced cell death (TUNEL) and microglia infiltration in USSC infused IVH pups compared to IVH-saline injected control. **(A–H):** Representative TUNEL labeling of the cryosections at postnatal day 3, images taken from periventricular area. The sections were counter stained with propidium iodide (nuclear). (A, E): Cryosections showed less number of TUNEL positive cells in the periventricular area of pups with no IVH control. (B, F): Higher number of TUNEL positive cells in IVH saline control. (C, G; D, H): The cryosections from ICV, IV USSC injected pups with IVH showed significantly reduced TUNEL positive cells at postnatal day 3 respectively. **(I):** The mean cell density of TUNEL positive nuclei was significantly increased in IVH saline pups compared with no IVH healthy controls, whereas in ICV, IV USSC-injected pups with IVH significantly reduced mean TUNEL positive cell density in the ventricular zone. The subventricular zone (SVZ) and periventricular zone (PVZ) the counts included cells in the germinal matrix (GM), corona radiata (CR), and corpus callosum (CC). All scale bars for the images 100 μm. TUNEL +nuclei (green), PI (red). Samples size 5–6 in each group. *,$p < .01$ for both no IVH controls versus IVH saline vehicle controls; *,$P < .05$ IVH saline controls versus ICV, IV USSC pups. **(J–L):** Representative immunofluorescence image labeled with Iba-1 specific antibody for microglia at postnatal day 3. The images were taken at CR. The sections were counter stained with diamidino-phenylindole (nuclear). (J, K): The cryosections showing high density of microglia in IVH pups compared with no IVH controls and the mean cell density between the groups was significant. (L): The ICV USSC pups with IVH showed significantly reduced microglia infiltration compared with Saline IVH controls at postnatal day 3. All scale bars for the images 100 μm. Abbreviations: DAPI, diamidino-phenylindole; ICV, intracerebroventricular; IVH, intraventricular hemorrhage; TUNEL, transferase dUTP nick-end labeling; USSC, unrestricted somatic stem cell.

treatment with USSCs via the ICV route in IVH showed partially improved length, number, and morphology of myelin fibers in the CR (Fig. 4E, 4F vs. 4C, 4D).

To further evaluate our observation of myelin recovery in IHC, we measured myelin mRNA expression by real time PCR using total RNA. MBP mRNA was significantly reduced in IVH pups compared with controls ($p < .05$; Fig. 6A). Notably, USSC administration significantly increased myelin mRNA levels at day 14 (Fig. 6A). These data suggest that USSC treatment not only helps restore morphology of myelin fibers but also enhances MBP gene expression by day 14.

USSC ICV Infusion Does Not Reduce Astrogliosis but Alters the Morphological Appearance of Astrocytes

Since reactive gliosis is a common finding in IVH, we compared the magnitude of astrogliosis among three groups of pups in a similar manner to our myelin assessment. GFAP-labeled coronal sections were evaluated for morphological changes of astrocyte processes and shape in the CR and GM at day 14 (Fig. 5A–5F). Consistent with our earlier data, GFAP immunoreactivity was higher showing less complex, thicker, shorter, fewer astrocyte processes in the CR of IVH pups compared to more complex, longer, and multiple thinner processes in no IVH controls (Fig. 5A, 5B vs. 5C, 5D). Reactive astrocytes visualized in IVH pups (Fig. 5C, 5D) was similar to the A1 astrocytes induced by neuroinflammatory microglia and cytokines reported by Liddelow et al. [38] and in our recent publication. [33] In contrast, USSC treatment resulted in an altered phenotype of GFAP-positive astrocytes with little or no astrocyte process (Fig. 5E, 5F).

To determine whether USSCs altered glial activation by microglia, we double labeled the coronal section with GFAP
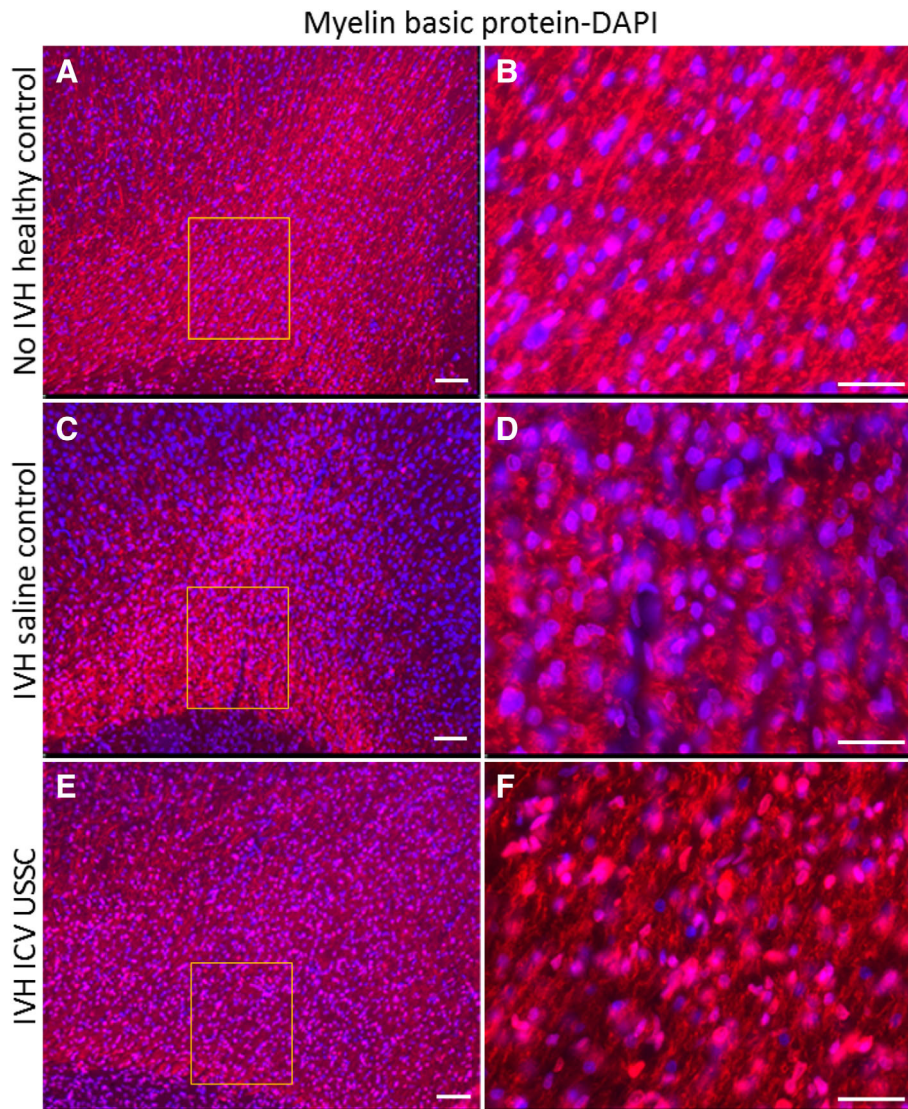
Myelin basic protein-DAPI

Figure 4. ICV USSC administration preserves myelin after IVH in premature rabbit pups. **(A–F):** Representative immunofluorescence images for myelin basic protein (MBP) in the corona radiata at postnatal day 14. (A, B): Thick and long myelinated fibers in rabbit pups without IVH controls (×10 and boxed area in high magnification in ×40). (C, D): Reduced and sparse of myelinated fibers with less density in IVH saline control pups (×10 and boxed area in high magnification in ×40). (E, F): The ICV USSC injected pups with IVH showed partial recovery of myelin fiber formation with more number of MBP positive cells (×10 and boxed area in high magnification in ×40). All images were taken from corona radiata (20 μm coronal sections) Samples size 5–6 in each group. All scale bars for the images 100 μm. Abbreviations: DAPI, diamidino-phenylindole; ICV, intracerebroventricular; IVH, intraventricular hemorrhage; USSC, unrestricted somatic stem cell.

and Iba-1 (GM shown in Fig. S5). As expected the huge number of morphologically different microglia (red) presented along with astrocytes in IVH pups compared to controls (Fig. S5A, S5B vs. S5C, S5D). Interestingly, we do not observe similar reactive astrocytes after USSC administration even in the GM (Fig. S5A–S5D vs. S5E, S5F). These data indicate that astrocytes after USSC treatment are morphologically different in both CR and GM compared to controls with or without IVH.

To assess the magnitude of expression of GFAP as indicative of astrogliosis, we measured GFAP mRNA and protein expression. The mRNA levels of GFAP were significantly increased in both IVH pups with and without USSC injection compared to healthy controls ($p < .05$, Fig. 6(B)). Similar results were also observed in GFAP-protein expression by protein analysis ($p < .05$, Fig. 6C). Interestingly, GFAP mRNA and

protein levels were comparable in IVH pups with and without USSC treatment.

Reduced IL-β and TNF-α in IVH Pups After USSC ICV Administration

Cytokines are known to play a key role in initiation, progression, and/or suppression of inflammatory reactions under pathological states. To determine whether USSCs affected cytokine expression in IVH-induced inflammation, we measured mRNA expression of relevant cytokines in our rabbit model of IVH: IL1-β and TNFα using qPCR. Consistent with our previous reports, [14, 39] the mRNA levels of IL1-β and TNF-α were significantly elevated in pups with IVH compared with no IVH controls at day 3 (Fig. 6D, 6E; $p < .05$). In contrast, USSC
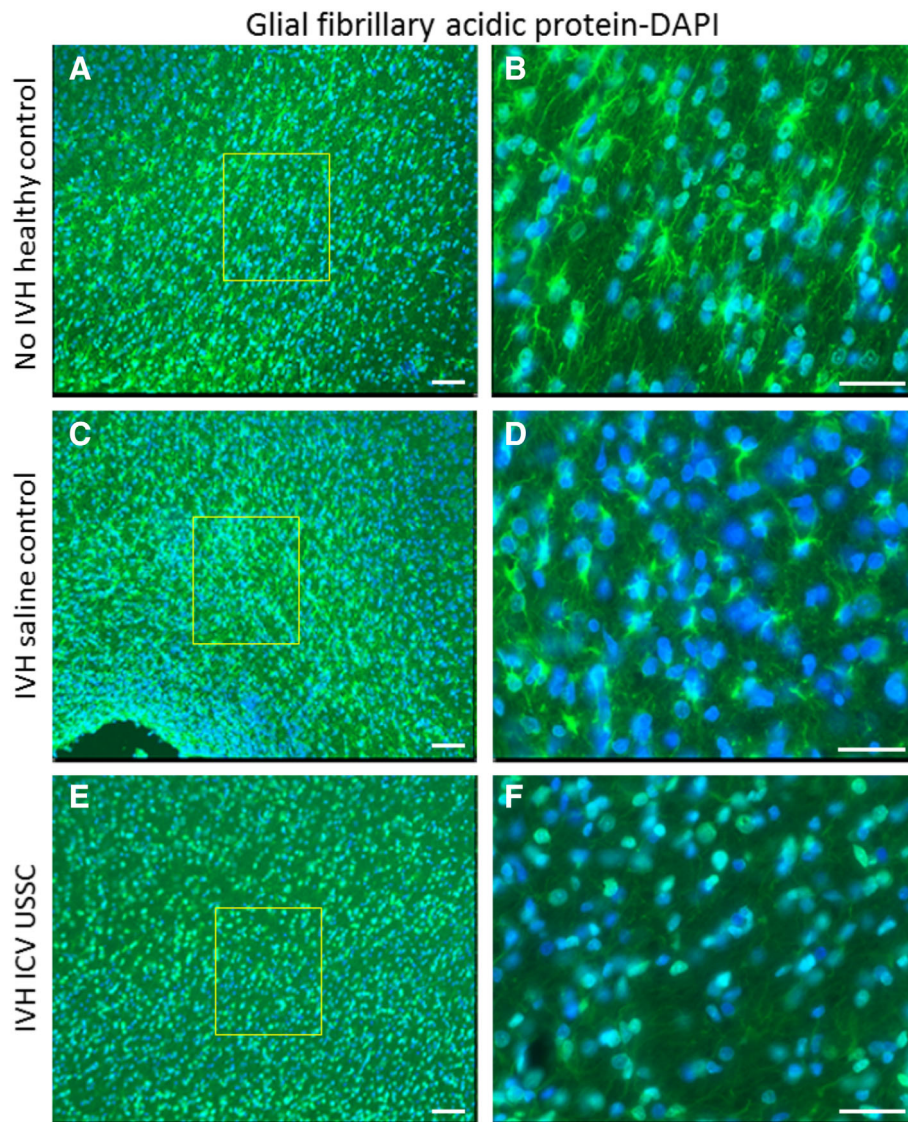
Glial fibrillary acidic protein-DAPI

Figure 5. Representative immunofluorescence of cryosections labeled with Glial fibrillary acidic protein (GFAP)-specific antibody at postnatal day 14 rabbit pups. **(A, B):** Thin and long astrocyte process with small cell body astrocytes with complex morphological appearance in no IVH rabbit pups (×10 and ×40 magnification). **(C, D):** Higher immunoreactivity with abundant hypertrophic astrocytes with small and thick astrocyte process with simple morphology in vehicle treated IVH pups (×10 and ×40 magnification) compared with no IVH healthy controls in the corona radiata of the lateral ventricle. **(E, F):** Abundant GFAP-positive astrocytes majorly with small cell body and some or no astrocyte process noted in the IVH pups injected with USSCs at day 14. All images were taken from corona radiata (20 μm coronal sections) Samples size 5–6 in each group. All scale bars for the images 100 μm. Abbreviations: DAPI, diamidino-phenylindole; ICV, intracerebroventricular; IVH, intraventricular hemorrhage; USSC, unrestricted somatic stem cell.

ICV injection significantly reduced IL1-β and TNF-α mRNA levels in IVH pups ($p < .05$; Fig. 6D, 6E).

DISCUSSION

This pilot study is the first to test the effects of human USSCs on injury and recovery in a preterm animal model of IVH. [13, 14, 19] We demonstrated that regional or systemic administration of USSCs reduced CNS inflammatory cytokine expression, cell death and microglial infiltration, improved myelination and reduced the severity of hydrocephalus after IVH. In addition,

USSC treatment showed improvement in sensorimotor function compared to IVH-saline controls.

Human cord blood-derived USSCs were investigated since they are reported to be more primitive and possess a higher regenerative potential than MSCs. [21] Human cord blood-derived USSCs have higher differentiation capacities than MSCs and have been expressed to be precursors to MSCs. USSCs are a rare population of stem cells in cord blood and efficiency for generating USSCs from cord blood units has been reported to range between 25% and 50%. However, once established the cell culture from cord blood, USSCs can be easily developed as an off-shelf stem cell product as they have significantly higher cumulative population doublings than
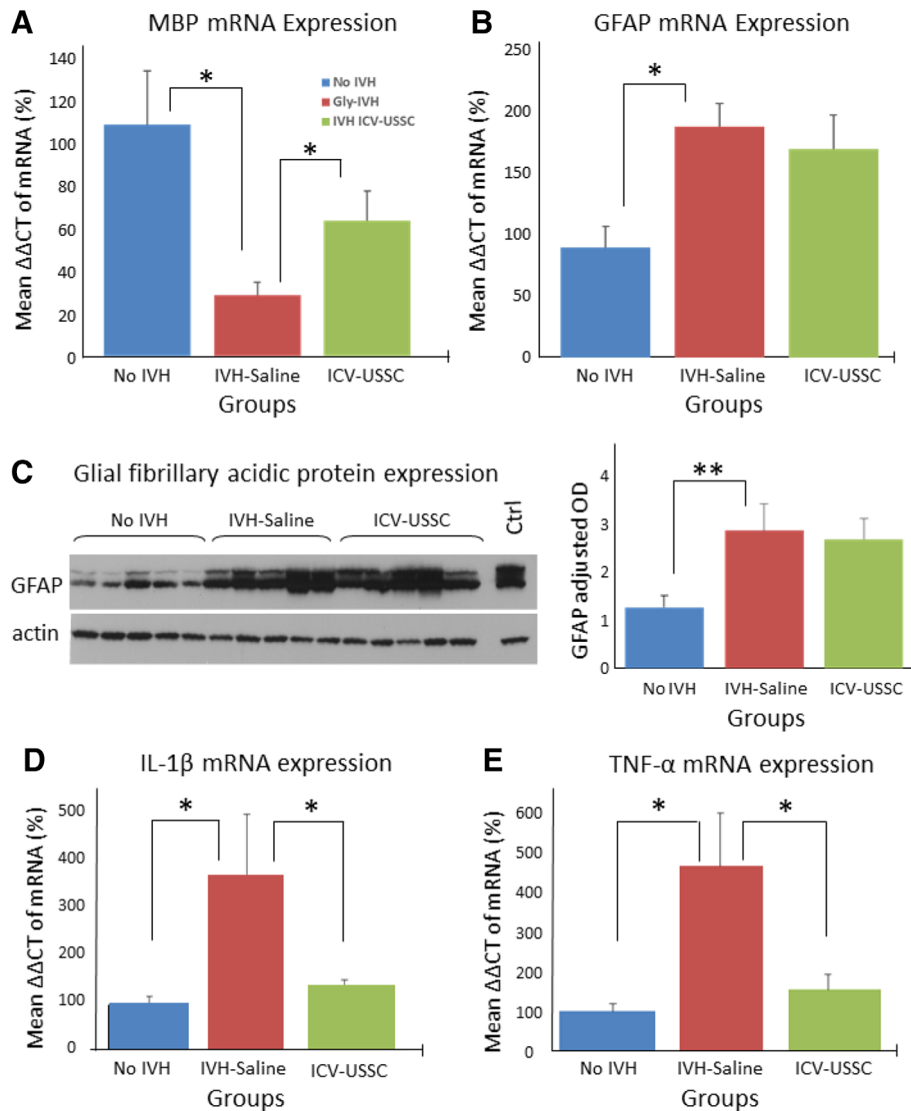
Figure 6. ICV administration of USSC altered the expression of myelin basic protein and proinflammatory cytokines but not glial fibrillary acidic protein after IVH. **(A):** Reduced myelin basic protein gene expression in IVH pups compared to without IVH control pups, whereas ICV USSC treated pups showed significantly recovered gene expression at postnatal day 14. (The data are mean ± SEM, n = 5–6 pups/group; $p < .05$ no IVH vs. IVH saline group as well as no IVH vs. ICV USSC pups with IVH.) **(B):** GFAP mRNA was higher in pups with IVH saline control compared to no IVH healthy controls at postnatal day 14. Importantly, after USSC administration, the GFAP mRNA expression was comparable in IVH pups with and without USSCs. (The data are mean ± SEM, n = 5–6 pups/group; $p < .05$ no IVH vs. IVH saline group.) **(C):** Representative western blot analysis of GFAP protein in the forebrain of the no IVH pups and IVH pups with and without USSC at postnatal day 14. Similar changes of GFAP gene expression that we have observed in qPCR, the protein expression was also elevated in IVH pups with and without USSCs compared to no IVH healthy controls. (Data are mean ± SEM, n = 5 pups/group, **$p < .01$.) The bar graph represents the adjusted OD normalized with beta actin. **(D, E):** ICV USSC administration suppressed IL-1β and TNF-α mRNA levels in intraventricular hemorrhage. IL-1β and TNF-α mRNA expression was assessed by real-time PCR, the total RNA was made from forebrain coronal slice in the no IVH controls, vehicle treated IVH and USSC treated IVH pups at postnatal day 3. (Data are mean ± SEM, n = 5–6 pups/group.) The IL-1β and TNF-α mRNA was higher in pups with IVH saline compared to no IVH controls at day 3 (*$p < .05$), whereas ICV USSC injected pups with IVH showed significant reduction in IL-1β and TNF-α mRNA expression (*$p < .05$). Abbreviations: GFAP, Glial fibrillary acidic protein; ICV, intracerebroventricular; IVH, intraventricular hemorrhage; OD, optical density; USSC, unrestricted somatic stem cell.

either cord blood- or bone marrow-derived MSCs without spontaneous differentiation. At passage 4, 1,500 million USSC cells can be obtained after expansion under GMP grade conditions. This is a great advantage of using USSCs as a cellular product rather than MSCs. Additionally, USSCs secrete a spectrum of trophic factors promoting neurite growth. USSCs also demonstrated the ability to migrate to the site of injury and antagonize TGFβ signaling-induced fibrosis and decrease

deposition of ECM components and expression of multiple MMPs in an inherited skin blistering disease (RDEB). [32] The results from this study demonstrate that USSCs are also an effective stem cell type for the treatment of IVH. Moreover, USSCs are attractive for clinical-translational potential as they can be purified and expanded without ethical concerns using good manufacturing practice (GMP)—grade procedures. [40]

In the current report, the ability to observe neuromotor effects of injected USSCs correlates with their survival and migration using noninvasive imaging techniques (IVIS-BLI) *in lieu* of other technology such as MRI shows promise for future tracking of USSCs as part of preclinical studies for at least 14 days postnatal age. Our pilot data are encouraging but future work requires longer duration studies to fully assess the potential for cellular integration and differentiation, as well as procedural refinements that better define optimal dose and frequency of USSC interventions to maximize beneficial effects.

Previous preclinical investigations of stem cell therapy for IVH focused primarily on MSCs in neonatal and adult animal models established by injection of *exogenous* blood. [8, 9, 11, 41, 42] The ICV and IV administration used in MSC studies and the persistence of injected cells assessed by IHC was not systematically tracked for sequential survival and migration or there was no evidence of engraftment in the brain. [8, 9, 41, 42] In contrast to prior work, our report is the first to demonstrate the survival and migration of regional or systemically injected stem cells into an injured premature brain by applying live imaging and IHC staining in combination. USSCs migrated to the site of injury, promoted wound healing and prevented fibrosis in animal models of RDEB. [24] Moreover, in both spinal cord injury (SCI) and RDEB, migration and persistence of USSCs at the injury site was evident yet, in only the RDEB model was epithelial-like differentiation observed. [24, 43]

To maximize the potential for clinical translation, we sought to identify whether differences existed in brain barrier effectiveness attributed to the route of administration by comparing IV to ICV treatments. Cell intensity in the brain was maximal on day 3 and persisted until day 7 using the IV route including widespread and earlier CNS parenchymal localization than observed with ICV cell placement which resulted in early aggregate "rosette" formation. Based on the observed histology, we speculate that the migration delay from the ventricle may be due to the formation of USSC aggregates with inflammatory cells of the ventricular blood prior to subsequent migration into the brain parenchyma; significantly, no USSC were detected in other organs after ICV injection.

In contrast to the ICV route, after IV infusion, BLI signal in the lung was initially intense and raised concern that entrapment of cells would compromise lung function (respiratory deterioration was not seen in our series) and mitigate CNS access. Fortunately, the absence of BLI signaling, except in the lung and injured brain suggested that stem cells were not sequestered in other un-injured organs (Fig. 1G). Our observations are analogous to those reported using IV MSCs in the *exogenous* blood IVH-mouse model (day 5) where IVIS-BLI signal was initially expressed in the lung and also remained until day 14. [11] Using either route of administration, most of the USSCs resided in the subventricular zone. No evidence was procured to support integration and differentiation of USSCs; this is similar to CNS reports after spinal cord injury. [43]

After IV administration, USSCs were more diffusely distributed in the subventricular zone and the periventricular injury region at least 2–3 days earlier than when administered by ICV injection (Fig. S2). We speculate that this illustrates an important therapeutic translational advantage for treatment of a global brain injury due to insults like hypoxia-ischemia rather than focal injury like a stroke. Another interpretation argues

that the ICV route causes USSCs to remain in the ventricles longer and that may have helped to reduce or alter the ventricular inflammatory process as the antecedent to hydrocephalus. Although being interesting speculations, our data did not illustrate significant differences in sensorimotor recovery or improved hydrocephalus following IVH using either route of treatment. This is encouraging, as an IV route would be preferred for the potential use in humans (Table 1). Importantly, we have not performed any experiments to demonstrate the mechanisms that underlie USSCs crossing the blood brain barrier (BBB). One of the possibilities in our rabbit model, the essential pathological feature of GMH-IVH, is disruption of the BBB due to fragile endothelium and immature pericyte coverage in the GM. [44] Failure of the BBB results in the leakage of vessels and causes edema that may allow for migration of USSC into the brain parenchyma. Similarly, the BBB in premature infants may be in the developing stage. Furthermore, compared to other sources for stem cell therapy such as bone marrow cells for CNS therapy, USSCs showed lower immunogenicity, possibly enabling them to cross an intact BBB. USSCs have the ability to migrate to the wound or injury; they express many chemokine receptors such as CXCL12 (for SDF1), PDGFR (for HMGB1), and CCR2 (for CCL7), [31] which might direct their specific migration to the site of injury. It is also important to mention that the localization of USSCs in the brain after IV injection is not randomly dispersed; it follows a trajectory path. Certain chemokines in the brain might induce specific trajectory of USSC migration. There were reports on mononuclear cells getting into the brain in animal models of stroke or HIE; however, those cells appeared to be random.

Administration of USSCs in both ICV and IV routes significantly reduced apoptosis and microglia infiltration in the ventricular zone (Fig. 3); IL1β and TNFα mRNA levels were also reduced (Fig. 6D, 6E). Given the neurological outcome of IVH in preterm animals is principally determined by the severity of hemorrhage and extent of parenchymal damage, we speculate that lowered levels of apoptosis, fewer microglia and lower cytokines indicate USSCs are acting primarily via a paracrine effect to mitigate injury. [45–47] Future work will be needed to fully characterize this process and its duration.

IVH-induced white matter injury is associated with cerebral palsy, hydrocephalus, and mental retardation. Cytokines IL1-β and TNF-α are tightly regulated in their expression and found to be at very low levels during postnatal brain development. [48–50] Following brain injury in either adult or developing animals, over expression of IL1-β, TNF-α, IL6, and IL8 by neurons, reactive astrocytes and microglia is characteristic. [49, 51–53] In our previous studies, we demonstrated suppression of inflammation followed by improved myelination and less gliosis using various pharmacological approaches indicating some degree of injury was reversible. [12, 14, 39, 54] Therefore, in the present study, we examined the same regions of the CR and CC (Fig. S4). In the current report, IVH pups showed upregulation of IL1-β and TNF-α mRNA (Fig. 6D, 6E) suggesting a role of activated microglia in inducing A1 reactive astrocytes similar to findings of A1 and A2 astrocytes in a LPS inflammation model. [38] USSC suppressed IL1-β and TNF-α and was associated with a partial reversal of altered astrocyte morphology. USSCs represent a multipotent CD45-negative population from human cord blood. In silico target gene predictions showed a large set of proteins involved in neuronal

differentiation and differentiation-related pathways such as axon guidance and TGFβ, WNT, and MAPK signaling. [55] Our data were too short to test for specific signaling mechanisms despite the fact that we observed significant reduction in inflammation and white matter injury correlating with improved neuromotor function. Previously, we have shown in our IVH model that IL-1β and TNF-α suppression will improve white matter injury through TNF mediated inflammatory cascade. [14] Therefore, we speculate that USSCs might have shown a paracrine effect similarly in this TNF inflammatory cascade. Alternately, the USSCs also had functional effect through exosome pathways by secreting neurotropic growth factors and initiating a paracrine effect, which mitigates injury caused by IVH. The USSC administration included morphologically improved myelin fibers in the CR and also increased MBP gene mRNA levels in the forebrain which may contribute to the improved motor function (Figs. 4 and 6A).

There are several limitations of this report, including the use of a single treatment time point and a fixed cell dosing regimen. Since injury and recovery evolve over time, a case can be made that multiple interventions are necessary along with varying the number of cells to be administered, to maximize potential benefits or that prophylactic intervention would provide further benefit. Longer safety follow-up is needed.

CONCLUSION

In summary, this is the first report that shows that administration of human USSCs in a premature-rabbit pup IVH model was associated with sensorimotor recovery, reduced apoptotic cell death, and less inflammatory cell infiltration and cytokine expression. USSC treatment was also associated with partial recovery of myelination and restoration/preservation of white matter structure, which may contribute directly to resumption of motor function. These findings support the possibility that USSCs exert a paracrine anti-inflammatory effect that mitigates the detrimental consequences of IVH, raising the translational potential for using USSCs for the treatment of premature infants with IVH.

AUTHOR CONTRIBUTIONS

G.V: conception, design, performed experiments, assembly, analysis, interpretation of the data and wrote the manuscript; E.F.L, M.S.C: Conception, data interpretation, manuscript writing, financial support, and approval of the manuscript; Y.L, L.I: USSC isolation, labeling and BLI imaging; F.H, D.P, D.A.F, P.B: animal care, sample collection, immunostaining, cell count, neurobehavioral study; S.S, M.T.Z, K.H: neurobehavioral study, cell count, imaging.

DISCLOSURE OF POTENTIAL CONFLICTS OF INTEREST

The authors indicated no potential conflicts of interest.

REFERENCES

1 Courtney SE, Durand DJ, Asselin JM et al. High-frequency oscillatory ventilation versus conventional mechanical ventilation for very-low-birth-weight infants. N Engl J Med 2002;347:643–652.

2 Horbar JD, Badger GJ, Carpenter JH et al. Trends in mortality and morbidity for very low birth weight infants, 1991-1999. Pediatrics 2002;110:143–151.

3 Lantos JD, Lauderdale DS. What is behind the rising rates of preterm birth in the United States? Rambam Maimonides Med J 2011;2:e0065.

4 Armstrong DL, Sauls CD, Goddard-Finegold J. Neuropathologic findings in short-term survivors of intraventricular hemorrhage. Am J Dis Child 1987;141:617–621.

5 Back SA. Perinatal white matter injury: The changing spectrum of pathology and emerging insights into pathogenetic mechanisms. Ment Retard Dev Disabil Res Rev 2006;12:129–140.

6 Rodríguez-Yáñez M, Castillo J. Role of inflammatory markers in brain ischemia. Curr Opin Neurol 2008;21:353–357.

7 Hailer NP. Immunosuppression after traumatic or ischemic CNS damage: It is neuroprotective and illuminates the role of microglial cells. Prog Neurobiol 2008;84:211–233.

8 Ahn SY, Chang YS, Sung DK et al. Mesenchymal stem cells prevent hydrocephalus after severe intraventricular hemorrhage. Stroke 2013;44:497–504.

9 Ahn SY, Chang YS, Park WS. Mesenchymal stem cells transplantation for neuroprotection in preterm infants with severe intraventricular hemorrhage. Korean J Pediatr 2014;57:251–256.

10 Liu AM, Lu G, Tsang KS et al. Umbilical cord-derived mesenchymal stem cells with forced expression of hepatocyte growth factor enhance remyelination and functional recovery in a rat intracerebral hemorrhage model. Neurosurgery 2010;67:357–365. discussion 365–356.

11 Mukai T, Mori Y, Shimazu T et al. Intravenous injection of umbilical cord-derived mesenchymal stromal cells attenuates reactive gliosis and hypomyelination in a neonatal intraventricular hemorrhage model. Neuroscience 2017;355:175–187.

12 Ballabh P, Xu H, Hu F et al. Angiogenic inhibition reduces germinal matrix hemorrhage. Nat Med 2007;13:477–485.

13 Chua CO, Chahboune H, Braun A et al. Consequences of intraventricular hemorrhage in a rabbit pup model. Stroke 2009;40:3369–3377.

14 Vinukonda G, Csiszar A, Hu F et al. Neuroprotection in a rabbit model of intraventricular haemorrhage by cyclooxygenase-2, prostanoid receptor-1 or tumour necrosis factor-alpha inhibition. Brain 2010;133:2264–2280.

15 Gram M, Sveinsdottir S, Cinthio M et al. Extracellular hemoglobin - Mediator of inflammation and cell death in the choroid plexus following preterm intraventricular hemorrhage. J Neuroinflammation 2014;11:200.

16 Ley D, Romantsik O, Vallius S et al. High Presence of Extracellular Hemoglobin in the Periventricular White Matter Following Preterm Intraventricular Hemorrhage. Front Physiol 2016;7:330.

17 Ballabh P. Pathogenesis and prevention of intraventricular hemorrhage. Clin Perinatol 2014;41:47–67.

18 Ballabh P, LaGamma EF. Strategies for working with a preterm rabbit model of glycerol-induced intraventricular hemorrhage: Strengths and limitations. Pediatr Res 2014;76:495–496.

19 Georgiadis P, Xu H, Chua C et al. Characterization of acute brain injuries and neurobehavioral profiles in a rabbit model of germinal matrix hemorrhage. Stroke 2008;39:3378–3388.

20 Vose LR, Vinukonda G, Jo S et al. Treatment with thyroxine restores myelination and clinical recovery after intraventricular hemorrhage. J Neurosci 2013;33:17232–17246.

21 Kogler G, Sensken S, Airey JA et al. A new human somatic stem cell from placental cord blood with intrinsic pluripotent differentiation potential. J Exp Med 2004;200:123–135.

22 Kogler G, Radke TF, Lefort A et al. Cytokine production and hematopoiesis supporting activity of cord blood-derived unrestricted somatic stem cells. Exp Hematol 2005;33:573–583.

23 Kluth SM, Buchheiser A, Houben AP et al. DLK-1 as a marker to distinguish unrestricted somatic stem cells and mesenchymal stromal cells in cord blood. Stem Cells Dev 2010;19:1471–1483.

24 Liao Y, Itoh M, Yang A et al. Human cord blood-derived unrestricted somatic stem cells promote wound healing and have therapeutic potential for patients with recessive dystrophic epidermolysis bullosa. Cell Transplant 2014;23:303–317.

25 Jin KL, Mao XO, Greenberg DA. Vascular endothelial growth factor: Direct neuroprotective effect in in vitro ischemia. Proc Natl Acad Sci U S A 2000;97:10242–10247.

26 Sun Y, Jin K, Xie L et al. VEGF-induced neuroprotection, neurogenesis, and angiogenesis after focal cerebral ischemia. J Clin Invest 2003;111:1843–1851.

27 Imitola J, Raddassi K, Park KI et al. Directed migration of neural stem cells to sites of CNS injury by the stromal cell-derived factor 1alpha/CXC chemokine receptor 4 pathway. Proc Natl Acad Sci U S A 2004;101:18117–18122.

28 Opatz J, Kury P, Schiwy N et al. SDF-1 stimulates neurite growth on inhibitory CNS myelin. Mol Cell Neurosci 2009;40:293–300.

29 Giacobini P, Messina A, Wray S et al. Hepatocyte growth factor acts as a motogen and guidance signal for gonadotropin hormone-releasing hormone-1 neuronal migration. J Neurosci 2007;27:431–445.

30 Ebens A, Brose K, Leonardo ED et al. Hepatocyte growth factor/scatter factor is an axonal chemoattractant and a neurotrophic factor for spinal motor neurons. Neuron 1996;17:1157–1172.

31 Liao Y, Ivanova L, Zhu H et al. Rescue of the mucocutaneous manifestations by human cord blood derived nonhematopoietic stem cells in a mouse model of recessive dystrophic epidermolysis bullosa. Stem Cells 2015; 33:1807–1817.

32 Liao Y, Ivanova L, Zhu H et al. Cord blood-derived stem cells suppress fibrosis and may prevent malignant progression in recessive dystrophic epidermolysis bullosa. Stem Cells 2018;36:1839–1850.

33 Vinukonda G, Hu F, Mehdizadeh R et al. Epidermal growth factor preserves myelin and promotes astrogliosis after intraventricular hemorrhage. Glia 2016;64:1987–2004.

34 Livak KJ, Schmittgen TD. Analysis of relative gene expression data using real-time quantitative PCR and the 2(−Delta Delta C(T)) method. Methods 2001;25:402–408.

35 Shitaka Y, Tran HT, Bennett RE et al. Repetitive closed-skull traumatic brain injury in mice causes persistent multifocal axonal injury and microglial reactivity. J Neuropathol Exp Neurol 2011;70:551–567.

36 Dohare P, Cheng B, Ahmed E et al. Glycogen synthase kinase-3beta inhibition enhances myelination in preterm newborns with intraventricular hemorrhage, but not recombinant Wnt3A. Neurobiol Dis 2018;118: 22–39.

37 Derrick M, Luo NL, Bregman JC et al. Preterm fetal hypoxia-ischemia causes hypertonia and motor deficits in the neonatal rabbit: A model for human cerebral palsy? J Neurosci 2004;24:24–34.

38 Liddelow SA, Guttenplan KA, Clarke LE et al. Neurotoxic reactive astrocytes are induced by activated microglia. Nature 2017; 541:481–487.

39 Dohare P, Zia MT, Ahmed E et al. AMPA-kainate receptor inhibition promotes neurologic recovery in premature rabbits with intraventricular hemorrhage. J Neurosci 2016; 36:3363–3377.

40 Aktas M, Buchheiser A, Houben A et al. Good manufacturing practice-grade production of unrestricted somatic stem cell from fresh cord blood. Cytotherapy 2010;12: 338–348.

41 Drobyshevsky A, Cotten CM, Shi Z et al. Human umbilical cord blood cells ameliorate motor deficits in rabbits in a cerebral palsy model. Dev Neurosci 2015;37:349–362.

42 Zhu W, Gao Y, Chang CF et al. Mouse models of intracerebral hemorrhage in ventricle, cortex, and hippocampus by injections of autologous blood or collagenase. PLoS One 2014;9:e97423.

43 Schira J, Gasis M, Estrada V et al. Significant clinical, neuropathological and behavioural recovery from acute spinal cord trauma by transplantation of a well-defined somatic stem cell from human umbilical cord blood. Brain 2012;135:431–446.

44 Ballabh P. Intraventricular hemorrhage in premature infants: mechanism of disease. Pediatr Res 2010;67:1–8.

45 Brouwer A, Groenendaal F, van Haastert IL et al. Neurodevelopmental outcome of preterm infants with severe intraventricular hemorrhage and therapy for post-hemorrhagic ventricular dilatation. J Pediatr 2008;152:648–654.

46 Bae SH, Kong TH, Lee HS et al. Long-lasting paracrine effects of human cord blood cells on damaged neocortex in an animal model of cerebral palsy. Cell Transplant 2012; 21:2497–2515.

47 Rosenkranz K, Meier C. Umbilical cord blood cell transplantation after brain ischemia-- From recovery of function to cellular mechanisms. Ann Anat 2011;193:371–379.

48 Silverstein FS, Barks JD, Hagan P et al. Cytokines and perinatal brain injury. Neurochem Int 1997;30:375–383.

49 Hagberg H, Gilland E, Bona E et al. Enhanced expression of interleukin (IL)-1 and IL-6 messenger RNA and bioactive protein after hypoxia-ischemia in neonatal rats. Pediatr Res 1996;40:603–609.

50 Szaflarski J, Burtrum D, Silverstein FS. Cerebral hypoxia-ischemia stimulates cytokine gene expression in perinatal rats. Stroke 1995;26:1093–1100.

51 Bartholdi D, Schwab ME. Expression of pro-inflammatory cytokine and chemokine mRNA upon experimental spinal cord injury in mouse: An in situ hybridization study. Eur J Neurosci 1997;9:1422–1438.

52 Streit WJ, Semple-Rowland SL, Hurley SD et al. Cytokine mRNA profiles in contused spinal cord and axotomized facial nucleus suggest a beneficial role for inflammation and gliosis. Exp Neurol 1998;152:74–87.

53 Zhang Z, Chopp M, Goussev A et al. Cerebral vessels express interleukin 1beta after focal cerebral ischemia. Brain Res 1998;784:210–217.

54 Dummula K, Vinukonda G, Chu P et al. Bone morphogenetic protein inhibition promotes neurological recovery after intraventricular hemorrhage. J Neurosci 2011;31: 12068–12082.

55 Iwaniuk KM, Schira J, Weinhold S et al. Network-like impact of MicroRNAs on neuronal lineage differentiation of unrestricted somatic stem cells from human cord blood. Stem Cells Dev 2011;20:1383–1394.

See www.StemCellsTM.com for supporting information available online.